QCD analysis of the P-wave charmonium electromagnetic Dalitz decays $h_c \to \eta^{(\prime)}\ell^+\ell^-$

Chao-Jie Fan and Jun-Kang He*

College of Physics and Electronic Science, Hubei Normal University, Huangshi 435002, China

(Received 26 January 2024; accepted 7 March 2024; published 5 April 2024)

The P-wave charmonium electromagnetic Dalitz decays $h_c \to \eta^{(\prime)}\ell^+\ell^-$ ($\ell = e, \mu$) with large recoil momentum are investigated in the framework of perturbative QCD, and the contributions from the small-recoil-momentum region are described by the overlap of soft wave functions. The transition form factors $f_{h_c\eta^{(\prime)}}(q^2)$ and the normalized transition form factors $F_{h_c\eta^{(\prime)}}(q^2)$ in full kinematic region are derived for the first time. It is noticed that there are no IR divergences at the one-loop level, and the transition form factors with the relativistic corrections from the internal momentum of h_c are insensitive to both the shapes of $\eta^{(\prime)}$ distribution amplitudes and the invariant mass of the lepton pair in the large-recoil-momentum region. Intriguingly, unlike the situation in the S-wave charmonium decays $J/\psi \to \eta^{(\prime)}\ell^+\ell^-$, we find that the contributions from the small-recoil-momentum region are comparable with those from the large-recoil-momentum region in the P-wave charmonium decays $h_c \to \eta^{(\prime)}\ell^+\ell^-$. By employing the obtained $F_{h_c\eta^{(\prime)}}(q^2)$, we give predictions of the branching ratios $\mathcal{B}(h_c \to \eta^{(\prime)}\ell^+\ell^-)$, which may come within the range of measurement of present or near-future experiments.

DOI: 10.1103/PhysRevD.109.074003

I. INTRODUCTION

The electromagnetic (EM) Dalitz decays of charmonia have received a great deal of attention in the last decade both experimentally [1–9] and theoretically [10–16], since they provide an ideal platform to probe the intrinsic structure of the charmonia and to study the fundamental mechanisms of the interactions between photons and hadrons [17,18]. One of the most interesting topics related to these EM Dalitz decays is the decay of charmonia to the mesons $\eta^{(\prime)}$, since it is directly related to the issue of η-η' mixing, which could offer new opportunities to study the $U(1)_A$ anomaly [19–27] and the $SU(3)_F$ breaking [25–29]. Under the classic assumption of pointlike particles [18,30], the EM Dalitz decays $J/\psi(\psi') \to \eta^{(\prime)}\ell^+\ell^-$ can be described by quantum electrodynamics (QED). The transition form factors (TFFs) $f_{\psi\eta^{(\prime)}}(q^2)$, which reflect the deviation from the QED prediction [18,30], can provide the dynamical information of the EM structure arising at the $J/\psi(\psi(2S)) \to \eta^{(\prime)}$ transition vertex. Consequently, the TFFs $f_{\psi\eta^{(\prime)}}(q^2)$ may help to distinguish transition mechanisms based on different dynamical pictures, such as the simple pole approximation [10,13,14], the effective Lagrangian approach [11,16], dispersion theory [12], and quantum chromodynamics (QCD) analysis [15].

The P-wave charmonium h_c cannot be directly produced in e^+e^- collisions because of the quantum numbers $J^{PC} = 1^{+-}$, but it can be produced through $\psi(2S) \to \pi^0 h_c$ [31,32]. In recent years, many more decay modes of h_c have been searched for at BESIII [32–38]. Due to the negative C parity, the h_c most likely decays into a photon and a pseudoscalar meson η_c or η (η'), in which the radiative decays $h_c \to \gamma\eta^{(\prime)}$ have first been observed by the BESIII Collaboration using about 4×10^8 $\psi(2S)$ events [33]. So far, there have been around 3×10^9 $\psi(2S)$ events collected with the BESIII detector [39–41], and it represents about an order-of-magnitude increase in statistics. This provides a good opportunity to study the EM Dalitz decays $h_c \to \eta^{(\prime)}\ell^+\ell^-$, and their branching ratios can be reached by present or near-future experiments, especially for the η' channels (reaching 10^{-5}). These EM Dalitz decays could not only offer useful information to constrain theoretical models (as mentioned above) in the charmonium region, but also shed light on the transition mechanism of $h_c \to \eta^{(\prime)}$ and the η-η' mixing effects [25,42,43] in different kinematic regions. Besides this, they are more interesting for the P-wave charmonia decays. Generally, inclusive P-wave charmonia decays suffer from IR divergences in the color-singlet-state contributions with the zero-binding approximation [44–46], while similar IR divergences do not appear

*hejk@hbnu.edu.cn

in exclusive P-wave charmonia decays [47–50]. This may imply that effects beyond those contained in the derivative of the nonrelativistic wave function at the origin play a key role. Recently, it has been pointed out that the relativistic corrections from the internal momentum of h_c are extremely important in the decays $h_c \to \gamma\eta^{(\prime)}$ [51]. This indicates that relativistic corrections may also be important in the EM Dalitz decays $h_c \to \eta^{(\prime)}\ell^+\ell^-$ due to the same EM structure arising at the $h_c \to \eta^{(\prime)}$ transition vertex.

In this paper, one of the major concerns is to clarify the dynamical picture of the EM Dalitz decays $h_c \to \eta^{(\prime)}\ell^+\ell^-$ in different kinematic regions. Phenomenologically, there exist three types of contributions in the decay processes $h_c \to \eta^{(\prime)}\ell^+\ell^-$: (i) In the large-recoil-momentum region (i.e., the square of the invariant mass of the lepton pair $q^2 = m^2_{\ell^+\ell^-} \simeq 0$), the transition mechanism of $h_c \to \eta^{(\prime)}$ could be described by the perturbative QCD approach, which has been reliably employed to treat the corresponding radiative decays $h_c \to \gamma\eta^{(\prime)}$ [51,52]. We call this transition mechanism the hard mechanism. (ii) In the small-recoil-momentum region [i.e., the square of the invariant mass of the lepton pair $q^2 \simeq q^2_{\rm max} = (M_{h_c} - m_{\eta^{(\prime)}})^2$], the transition mechanism of $h_c \to \eta^{(\prime)}$ is governed by the overlapping integration of the soft wave functions, and this transition mechanism is the so-called wave function overlap [53–61] (i.e., the soft mechanism). The TFFs $f_{h_c\eta^{(\prime)}}(q^2)$ account for the size effects from the spatial wave functions of the initial- and final-state hadrons. (iii) In resonance regions, such as $q^2 \simeq m^2_\rho, m^2_\omega, m^2_\phi$, the transition mechanism of $h_c \to \eta^{(\prime)}$ can be universally described by the vector-meson dominance (VMD) model [62], in which the resonance interaction between photons and hadrons is predominant. However, on the one hand, the contributions from VMD are negligibly small due to the narrow widths of resonances (see Ref. [15] for more details), and on the other hand, there are still some open questions for the VMD model, such as the sign ambiguity in the amplitude from the intermediate vector mesons and the off-mass-shell effects of the coupling constants [63]. To make the dynamical picture of the EM Dalitz decays $h_c \to \eta^{(\prime)}\ell^+\ell^-$ clear, we will mainly present the detailed discussions about the hard mechanism and the soft mechanism in the later parts of this paper. In the large-recoil-momentum region, by employing the Bethe-Salpeter (B-S) framework [51,64–68], we work out the B-S wave function of h_c, in which the internal momentum is retained. Considering a large momentum transfer, one can adopt the light-cone distribution amplitudes (DAs) to describe the internal dynamics of the final light mesons $\eta^{(\prime)}$, and the involved quark-antiquark and gluonic contents of $\eta^{(\prime)}$ are taken into account in our calculations. By an analytic calculation of the involved one-loop integrals, we find that the TFFs $f_{h_c\eta^{(\prime)}}(q^2)$ are UV and IR safe, and they barely depend on the shapes of the light-meson DAs. Furthermore, the gluonic contributions and the quark-antiquark contributions are comparable in the TFFs $f_{h_c\eta^{(\prime)}}(q^2)$. It is compatible with the situation in the corresponding radiative decays $h_c \to \gamma\eta^{(\prime)}$ [51,52]. In the small-recoil-momentum region, the TFFs are calculated phenomenologically by the wave-function overlap. Through a detailed calculation, we obtain the TFFs $f_{h_c\eta^{(\prime)}}(q^2)$ in the whole kinematic region for the first time. It is worthwhile to point out that the contributions from the soft mechanism and those from the hard mechanism are comparable with each other in the branching ratios $\mathcal{B}(h_c \to \eta^{(\prime)}\ell^+\ell^-)$, unlike the situation in S-wave charmonium EM Dalitz decays $J/\psi \to \eta^{(\prime)}\ell^+\ell^-$ [15], where the soft contributions are suppressed because of the special form of the spin structure of their amplitudes. In order to remove the main uncertainties arising from the bound-state wave functions, we use the normalized TFFs $F_{h_c\eta^{(\prime)}}(q^2) \equiv f_{h_c\eta^{(\prime)}}(q^2)/f_{h_c\eta^{(\prime)}}(0)$ to obtain the predictions of the branching ratios $\mathcal{B}(h_c \to \eta^{(\prime)}\ell^+\ell^-)$.

The paper is organized as follows: The theoretical framework for the EM Dalit decays $h_c \to \eta^{(\prime)}\ell^+\ell^-$ is presented in detail in Sec. II. In Sec. III, we show our numerical results and some phenomenological discussions, and Sec. IV is our summary.

II. THEORETICAL FRAMEWORK

A. Hard mechanism

1. Contributions of the quark-antiquark content of $\eta^{(\prime)}$

In the large-recoil-momentum region of $\eta^{(\prime)}$, the EM Dalitz decays $h_c \to \eta^{(\prime)}\ell^+\ell^-$ can be described by the perturbative QCD approach. The leading-order Feynman diagrams for the quark-antiquark content of $\eta^{(\prime)}$ arise from one-loop QCD processes. One of them is illustrated in Fig. 1, and the other five diagrams come from permutations of the photon and the gluon legs. Here and in what follows, the involved kinematical variables are labeled in Fig. 1, where u and $\bar{u}$ are the momentum fractions carried by the light quark and the light antiquark, respectively. According to the Feynman diagrams, one can obtain the amplitude of $h_c \to \eta^{(\prime)}\ell^+\ell^-$,

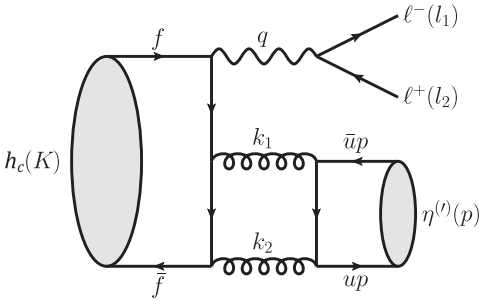

FIG. 1. One typical Feynman diagram for $h_c \to \eta^{(\prime)}\ell^+\ell^-$ with the quark-antiquark content of $\eta^{(\prime)}$, and the kinematical variables are labeled.

$$\mathcal{M} = -\frac{e}{q^2}\mathcal{A}^{\alpha\beta}\varepsilon_\alpha(K)\bar{u}(l_1)\gamma_\beta v(l_2), \tag{2.1}$$

where $\mathcal{A}^{\alpha\beta}$ represents the amplitude of $h_c \to \eta^{(\prime)}\gamma^*$; K and $\varepsilon(K)$ stand for the momentum and polarization vectors of h_c, respectively; q stands for the momentum of the virtual photon, while $q^2 = m^2_{\ell^+\ell^-}$ is the square of the invariant mass of the lepton pair; and l_1 and l_2 stand for the momenta of the leptons ℓ^- and ℓ^+, respectively.

It is convenient to convert the amplitude of $h_c \to \eta^{(\prime)}\gamma^*$ into two parts: the effective coupling of the process $h_c \to g^*g^*\gamma^*$, and that of the process $g^*g^* \to \eta^{(\prime)}$. By multiplying the two parts, inserting the gluon propagators, and performing the loop integrations, one can obtain the final amplitude of $h_c \to \eta^{(\prime)}\gamma^*$.

In the rest frame of the P-wave charmonium h_c, the amplitude of $h_c \to g^*g^*\gamma^*$ can be written as [69–71]

$$\begin{aligned}&\mathcal{A}_1^{\alpha\beta\mu\nu}\varepsilon_\alpha(K)\epsilon^*_\beta(q)\epsilon^*_\mu(k_1)\epsilon^*_\nu(k_2)\\ &= \sqrt{3}\int\frac{\mathrm{d}^4k}{(2\pi)^4}\mathrm{Tr}[\Psi(K,k)\mathcal{O}(f,\bar{f})],\end{aligned} \tag{2.2}$$

where $\Psi(K,k)$ represents the B-S wave function of h_c; $\mathcal{O}(f,\bar{f})$ represents the hard-scattering amplitude; $\sqrt{3}$ represents the color factor; $\epsilon(q)$ represents the polarization vector of the virtual photon; k_1, k_2 and $\epsilon(k_1)$, $\epsilon(k_2)$ represent the two gluons' momenta and polarization vectors; f and $\bar{f}$ represent the momenta of the quark c and antiquark $\bar{c}$; and they read

$$\begin{aligned}f^\mu &= \frac{K^\mu}{2} + k^\mu = \left(\frac{M}{2} + k^0, \mathbf{k}\right),\\ \bar{f}^\mu &= \frac{K^\mu}{2} - k^\mu = \left(\frac{M}{2} - k^0, -\mathbf{k}\right),\end{aligned} \tag{2.3}$$

with k being the relative momentum between the quark c and antiquark $\bar{c}$—i.e., the internal momentum of the P-wave charmonium h_c. Here, M is the mass of h_c. For convenience in subsequent calculations, we divide the internal momentum of h_c into two parts: the transverse component $\hat{k}$ with $\hat{k}\cdot K = 0$, and the longitudinal component $k_\parallel$ with $k_\parallel \cdot \hat{k} = 0$: i.e.,

$$k^\mu = k^\mu_\parallel + \hat{k}^\mu, \qquad k^\mu_\parallel = \frac{k_K}{M}K^\mu, \tag{2.4}$$

where both $k_K = \frac{k\cdot K}{M}$ and $\hat{k}^2 = k^2 - k_K^2$ are Lorentz-invariant variables. Considering the rest frame of h_c, one can easily know that $\hat{k}$ involves three degrees of freedom (namely, the component $\mathbf{k}$) orthogonal to the total momentum K, and k_K contains the remaining one degree of freedom (namely, the component k^0). Now, the volume element of the internal momentum k can be expressed in the form $\mathrm{d}^4k = \mathrm{d}^3\hat{k}\mathrm{d}k_K$. Furthermore, with a more relevant treatment where $k^0 \ll M$, we obtain the momenta

$$f^\mu \approx \left(\frac{M}{2}, \mathbf{k}\right) = \frac{K^\mu}{2} + \hat{k}^\mu, \quad \bar{f}^\mu \approx \left(\frac{M}{2}, -\mathbf{k}\right) = \frac{K^\mu}{2} - \hat{k}^\mu, \tag{2.5}$$

and the hard-scattering amplitude

$$\mathcal{O}(f,\bar{f}) \approx \mathcal{O}(\hat{k}), \tag{2.6}$$

and this treatment maintains the gauge invariance of the hard-scattering amplitude [72].

By employing the B-S equation [64,65] of the P-wave charmonium h_c, one can reduce the B-S equation to the Salpeter equation under the covariant instantaneous ansatz (CIA) [66–68]. The Salpeter wave function is defined as

$$\psi(\hat{k}) = \frac{i}{2\pi}\int \mathrm{d}k_K\Psi(K,k). \tag{2.7}$$

Subsequently, we obtain an analytic Salpeter wave function of h_c by solving the Salpeter equation (more details can be found in our recent investigation [51])

$$\psi(\hat{k}) = \hat{k}\cdot\varepsilon(K)\left[1 + \frac{\not{K}}{M} + \frac{\hat{k}\not{K}}{\hat{m}_c M}\right]\gamma^5 f(\hat{k}^2), \tag{2.8}$$

where $\hat{m}_c$ is the effective mass of the c quark, and the front factor $\hat{k}\cdot\varepsilon(K)$ indicates that the wave function is the nature of the P-wave, and the scalar function $f(\hat{k}^2)$ reads

$$f(\hat{k}^2) = N_A\left(\frac{2}{3}\right)^{\frac{1}{2}}\frac{1}{\pi^{\frac{3}{4}}\beta_A^{\frac{5}{2}}}|\hat{\mathbf{k}}|e^{-\frac{\hat{\mathbf{k}}^2}{2\beta_A^2}}, \tag{2.9}$$

with N_A being the normalization constant and β_A the harmonic oscillator parameter. The normalization equation of $f(\hat{q}^2)$ reads

$$\int\frac{\mathrm{d}^3\hat{k}}{(2\pi)^3}\frac{4\omega\hat{\mathbf{k}}^2}{3\hat{m}_c M}f^2(\hat{k}^2) = 1. \tag{2.10}$$

Using Eqs. (2.6) and (2.7), we can rewrite the amplitude of $h_c \to \gamma g^*g^*$:

$$\begin{aligned}&\mathcal{A}_1^{\alpha\beta\mu\nu}\varepsilon_\alpha(K)\epsilon^*_\beta(q)\epsilon^*_\mu(k_1)\epsilon^*_\nu(k_2)\\ &= -i\sqrt{3}\int\frac{\mathrm{d}^3\hat{k}}{(2\pi)^3}\mathrm{Tr}[\psi(\hat{k})\mathcal{O}(\hat{k})],\end{aligned} \tag{2.11}$$

where the hard-scattering amplitude $\mathcal{O}(\hat{k})$ reads

$$\begin{aligned}\mathcal{O}(\hat{k}) = iQ_c e g_s^2 \frac{\delta_{ab}}{6}\Bigg[&\epsilon^*(k_2)\frac{\frac{\not{K}_2-\not{q}-\not{K}_1}{2}+\hat{\not{k}}+m_c}{\left(\frac{k_2-q-k_1}{2}+\hat{k}\right)^2-m_c^2}\epsilon^*(q)\frac{\frac{\not{K}_2+\not{q}-\not{K}_1}{2}+\hat{\not{k}}+m_c}{\left(\frac{k_2+q-k_1}{2}+\hat{k}\right)^2-m_c^2}\epsilon^*(k_1)\\
&+\epsilon^*(k_1)\frac{\frac{\not{K}_1-\not{q}-\not{K}_2}{2}+\hat{\not{k}}+m_c}{\left(\frac{k_1-q-k_2}{2}+\hat{k}\right)^2-m_c^2}\epsilon^*(q)\frac{\frac{\not{K}_1+\not{q}-\not{K}_2}{2}+\hat{\not{k}}+m_c}{\left(\frac{k_1+q-k_2}{2}+\hat{k}\right)^2-m_c^2}\epsilon^*(k_2)\\
&+\epsilon^*(k_2)\frac{\frac{\not{K}_2-\not{K}_1-\not{q}}{2}+\hat{\not{k}}+m_c}{\left(\frac{k_2-k_1-q}{2}+\hat{k}\right)^2-m_c^2}\epsilon^*(k_1)\frac{\frac{\not{K}_2+\not{K}_1-\not{q}}{2}+\hat{\not{k}}+m_c}{\left(\frac{k_2+k_1-q}{2}+\hat{k}\right)^2-m_c^2}\epsilon^*(q)\\
&+\epsilon^*(q)\frac{\frac{\not{q}-\not{K}_2-\not{K}_1}{2}+\hat{\not{k}}+m_c}{\left(\frac{q-k_2-k_1}{2}+\hat{k}\right)^2-m_c^2}\epsilon^*(k_2)\frac{\frac{\not{q}+\not{K}_2-\not{K}_1}{2}+\hat{\not{k}}+m_c}{\left(\frac{q+k_2-k_1}{2}+\hat{k}\right)^2-m_c^2}\epsilon^*(k_1)\\
&+\epsilon^*(k_1)\frac{\frac{\not{K}_1-\not{K}_2-\not{q}}{2}+\hat{\not{k}}+m_c}{\left(\frac{k_1-k_2-q}{2}+\hat{k}\right)^2-m_c^2}\epsilon^*(k_2)\frac{\frac{\not{K}_1+\not{K}_2-\not{q}}{2}+\hat{\not{k}}+m_c}{\left(\frac{k_1+k_2-q}{2}+\hat{k}\right)^2-m_c^2}\epsilon^*(q)\\
&+\epsilon^*(q)\frac{\frac{\not{q}-\not{K}_1-\not{K}_2}{2}+\hat{\not{k}}+m_c}{\left(\frac{q-k_1-k_2}{2}+\hat{k}\right)^2-m_c^2}\epsilon^*(k_1)\frac{\frac{\not{q}+\not{K}_1-\not{K}_2}{2}+\hat{\not{k}}+m_c}{\left(\frac{q+k_1-k_2}{2}+\hat{k}\right)^2-m_c^2}\epsilon^*(k_2)\Bigg],\end{aligned} \tag{2.12}$$

with the c-quark mass m_c.

To proceed, we treat the light mesons $\eta^{(\prime)}$ as a light-cone object in the large-recoil-momentum region because of a large momentum transfer. Using the light-cone expansion, one can obtain the amplitude of $g^*g^* \to \eta^{(\prime)}$ [52,73–76]:

$$\begin{aligned}\mathcal{A}_2^{\mu\nu} = &-i(4\pi\alpha_s)\delta_{ab}\epsilon^{\mu\nu\rho\sigma}k_{1\rho}k_{2\sigma}\sum_{q=u,d,s}\frac{f^q_{\eta^{(\prime)}}}{6}\int_0^1 du\phi^q(u)\\
&\times\left(\frac{1}{\bar{u}k_1^2+uk_2^2-u\bar{u}m^2}+(u\leftrightarrow\bar{u})\right),\end{aligned} \tag{2.13}$$

where m represents the mass of $\eta^{(\prime)}$, the values $f^q_{\eta^{(\prime)}}$ are the decay constants, and $\phi^q(u)$ is the light-cone DA. The DA can be expressed as [52,77]

$$\phi^q(u) = 6u(1-u)\left[1+\sum_{n=2,4\cdots}c_n^q(\mu)C_n^{\frac{3}{2}}(2u-1)\right], \tag{2.14}$$

with $c_n^q(\mu)$ being the Gegenbauer moments, and we take three typical models listed in Table 1 of Ref. [52] (see Refs. [52,77] for more details). In our subsequent calculations, it is found that the TFFs $f_{h_c\eta^{(\prime)}}(q^2)$ are insensitive to the models of the light-cone DA. The decay constants $f^q_{\eta^{(\prime)}}$, in the quark-flavor basis, can be parametrized as [25,26,43,78,79]

$$\begin{aligned}f_\eta^{u(d)} &= \frac{f_q}{\sqrt{2}}\cos\phi, \qquad f_\eta^s = -f_s\sin\phi,\\
f_{\eta'}^{u(d)} &= \frac{f_q}{\sqrt{2}}\sin\phi, \qquad f_{\eta'}^s = f_s\cos\phi,\end{aligned} \tag{2.15}$$

where the phenomenological parameters (ϕ, f_q, and f_s) could be determined by different methods [11,25,51,52,76,80–85].

By contracting the above two amplitudes, inserting the gluon propagators, and integrating over the loop momentum, we obtain the decay amplitude of $h_c \to \eta^{(\prime)}\gamma^*$:

$$\mathcal{A}^{\alpha\beta} = \frac{1}{2}\int\frac{\mathrm{d}^4k_1}{(2\pi)^4}\mathcal{A}_1^{\alpha\beta\mu\nu}\mathcal{A}_{2\mu\nu}\frac{i}{k_1^2+i\epsilon}\frac{i}{k_2^2+i\epsilon}. \tag{2.16}$$

Considering parity conservation, Lorentz invariance, gauge invariance, and current conservation, one knows that

$$\mathcal{A}^{\alpha\beta} \propto \left(-g^{\alpha\beta}+\frac{q^\alpha K^\beta}{q\cdot K}\right). \tag{2.17}$$

Then, the $h_c \to \eta^{(\prime)}\gamma^*$ TFFs can be defined by

$$\mathcal{A}^{\alpha\beta} = -ef^Q_{h_c\eta^{(\prime)}}(q^2)\left(-g^{\alpha\beta}+\frac{q^\alpha K^\beta}{q\cdot K}\right). \tag{2.18}$$

With the help of the projection operator

$$\mathcal{P}^{\alpha\beta} = \left(2+\frac{M^2q^2}{(q\cdot K)^2}\right)^{-1}\left(-g^{\alpha\beta}+\frac{q^\alpha K^\beta}{q\cdot K}\right), \tag{2.19}$$

the TFFs can be rewritten as

$$f^Q_{h_c\eta^{(\prime)}}(q^2) = -e^{-1}\mathcal{P}_{\alpha\beta}\mathcal{A}^{\alpha\beta}. \tag{2.20}$$

Here, we show the expression of the TFFs more clearly:

$$f^{Q}_{h_c\eta^{(\prime)}}(q^2) = -\frac{i8\pi^2\alpha_s^2}{9\sqrt{3}}\sum_q f^q_{\eta^{(\prime)}}\int\frac{\mathrm{d}^3\hat{k}}{(2\pi)^3}\int \mathrm{d}u\phi^q(u) \times\int\frac{\mathrm{d}^4k_1}{(2\pi)^4}\left(\left(\frac{N_1}{D_1D_2D_3D_4}+\frac{N_2}{D_1D_2D_3D_{4p}} +\frac{N_3}{D_1D_2D_3D_5}+\frac{N_4}{D_1D_2D_3D_{5p}} +\frac{N_5}{D_1D_2D_3D_{4p}D_5}+\frac{N_6}{D_1D_2D_3D_4D_{5p}}\right) +(u\to\bar{u})\right), \tag{2.21}$$

with u and $\bar{u}=(1-u)$ being the momentum fractions arising from the light mesons $\eta^{(\prime)}$. The expressions of the denominators read

$$\begin{aligned} D_1 &= k_1^2+i\epsilon,\\ D_2 &= (k_1-p)^2+i\epsilon,\\ D_3 &= (k_1-up)^2+i\epsilon,\\ D_4 &= \left(k_1-\hat{k}+\frac{q-p}{2}\right)^2-m_c^2+i\epsilon,\\ D_{4p} &= \left(k_1+\hat{k}+\frac{q-p}{2}\right)^2-m_c^2+i\epsilon,\\ D_5 &= \left(k_1+\hat{k}-\frac{q+p}{2}\right)^2-m_c^2+i\epsilon,\\ D_{5p} &= \left(k_1-\hat{k}-\frac{q+p}{2}\right)^2-m_c^2+i\epsilon, \end{aligned} \tag{2.22}$$

and the expressions of the numerators $N_1\sim N_6$ are presented in the Appendix.

With the help of the algebraic identity ($u\neq 0,\ 1$)

$$\frac{D_1}{um^2}+\frac{D_2}{(1-u)m^2}-\frac{D_3}{u(1-u)m^2}=1, \tag{2.23}$$

the TFFs $f^{Q}_{h_c\eta^{(\prime)}}(q^2)$ can be decomposed into a sum of four-point and three-point one-loop integrals. When $u=0,\ 1$, the denominators of the propagators have the relation $D_3=D_1, D_2$, and the TFFs can also be decomposed into four-point or three-point integrals. Then, one can analytically evaluate these one-loop integrals with the technique proposed in Refs. [86–88] or the computer program PACKAGE-X [89,90]. It is found that the TFFs are UV and IR safe. Similarly to the situation in the radiative decays $h_c\to\gamma\eta^{(\prime)}$ [51,52], the TFFs are insensitive to the DAs of $\eta^{(\prime)}$. Our numerical results show that the change in the modulus of the TFFs does not exceed 1% with the different models of the DAs. Therefore, the theoretical uncertainties from the DAs are ignorable in our calculations of the TFFs, and we choose model I of the meson DA in Table 1 of Ref. [52].

2. Contributions of the gluonic content of $\eta^{(\prime)}$

Generally speaking, the contributions of the gluonic content of $\eta^{(\prime)}$ are expected to be small, because the gluonic content cloud be seen as higher-order effects from the point of view of the QCD evolution of the two-gluon DA, which vanishes in the asymptotic limit. For example, the gluonic contributions are strongly suppressed by the factor $m^2_{\eta^{(\prime)}}/M^2_{J/\psi}$ in the radiative decays $J/\psi\to\gamma\eta^{(\prime)}$ [76]. However, there is no suppression factor in the P-wave charmonium radiative decays $h_c\to\gamma\eta^{(\prime)}$ [51,52], due to the special form of the spin structure in their amplitudes. So, the gluonic contributions may become important in the radiative decays of the P-wave charmonium h_c. In fact, as pointed out in Refs. [51,52], the gluonic contributions and the quark-antiquark contributions are comparable with each other in the radiative decays $h_c\to\gamma\eta^{(\prime)}$. Obviously, this situation should be found in the large-recoil-momentum region of $\eta^{(\prime)}$ of the decays $h_c\to\eta^{(\prime)}\ell^+\ell^-$, due to the same spin structures in their hadronic matrix elements. The corresponding Feynman diagram is depicted in Fig. 2, and the other two diagrams arise from permutations of the photon and the gluon legs.

At the leading twist level, the matrix elements of the mesons $\eta^{(\prime)}$ over two-gluon fields in the light-cone expansion can be written as [77,91,92]

$$\langle\eta^{(\prime)}(p)|A^a_\alpha(x)A^b_\beta(y)|0\rangle = \frac{1}{4}\epsilon_{\alpha\beta\mu\nu}\frac{n^\mu p^\nu}{p\cdot n}\frac{C_F}{\sqrt{3}}\frac{\delta^{ab}}{8}f^1_{\eta^{(\prime)}} \times\int \mathrm{d}u e^{i(up\cdot x+\bar{u}p\cdot y)}\frac{\phi^g(u)}{u(1-u)}, \tag{2.24}$$

where $n=\frac{1}{\sqrt{2}}(1,-\frac{\mathbf{p}}{|\mathbf{p}|})$ is a lightlike vector along the opposite direction of the mesons $\eta^{(\prime)}$ [91], $f^1_{\eta^{(\prime)}}=\frac{1}{\sqrt{3}}(f^u_{\eta^{(\prime)}}+f^d_{\eta^{(\prime)}}+f^s_{\eta^{(\prime)}})$ are the effective decay constant, and the gluonic twist-2 DA is [77,92,93]

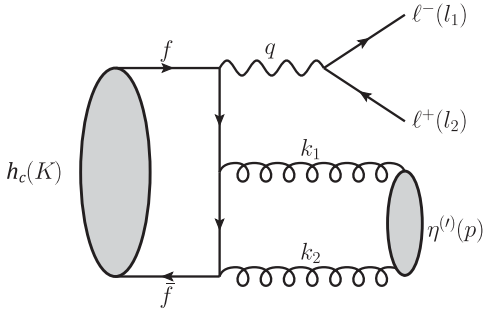

FIG. 2. One typical Feynman diagram for $h_c\to\eta^{(\prime)}\ell^+\ell^-$ with the gluonic content of $\eta^{(\prime)}$. The kinematical variables are labeled.

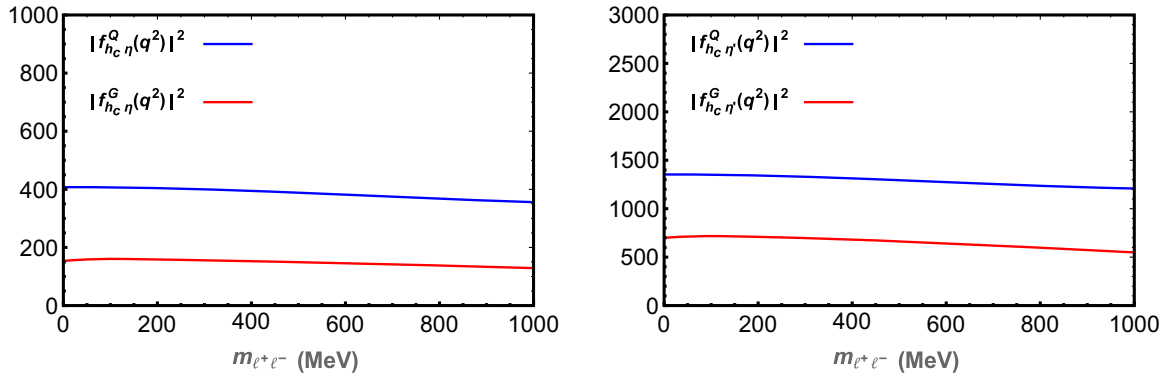

FIG. 3. The dependence of the modulus square of the TFFs $|f^{Q,G}_{h_c\eta^{(\prime)}}(q^2)|^2$ on the dilepton invariant mass $m_{\ell^+\ell^-}$ (or q^2).

$$\phi^g(u) = 30u^2(1-u)^2 \sum_{n=2,4\cdots} c_n^g(\mu) C_{n-1}^{\frac{5}{2}}(2u-1). \tag{2.25}$$

After a series of calculations, we obtain the corresponding TFFs $f^{G}_{h_c\eta^{(\prime)}}(q^2)$:

$$f^{G}_{h_c\eta^{(\prime)}}(q^2) = -\frac{16\pi\alpha_s}{27} f^1_{\eta^{(\prime)}} \int \mathrm{d}u \frac{\phi^g(u)}{u(1-u)} \int \frac{\mathrm{d}^3\hat{k}}{(2\pi)^3} \times \left(\frac{N_7}{C_1C_2} + \frac{N_8}{C_2C_3} + \frac{N_9}{C_3C_4}\right), \tag{2.26}$$

where the expressions of the denominators read

$$\begin{aligned} C_1 &= \left(\hat{k} + q - \frac{K}{2}\right)^2 - m_c^2 + i\epsilon, \\ C_2 &= \left(\hat{k} - \bar{u}p + \frac{K}{2}\right)^2 - m_c^2 + i\epsilon, \\ C_3 &= \left(\hat{k} + up - \frac{K}{2}\right)^2 - m_c^2 + i\epsilon, \\ C_4 &= \left(\hat{k} - q + \frac{K}{2}\right)^2 - m_c^2 + i\epsilon, \end{aligned} \tag{2.27}$$

and the expressions of the numerators $N_7 \sim N_9$ are presented in the Appendix.

Performing the integral calculations of the TFFs $f^{Q}_{h_c\eta^{(\prime)}}(q^2)$ and $f^{G}_{h_c\eta^{(\prime)}}(q^2)$, we find that the modulus square of these TFFs is very insensitive to the dilepton invariant mass $m_{\ell^+\ell^-}$ (or q^2). In Fig. 3, the $m_{\ell^+\ell^-}$ dependence of the modulus square $|f^{Q,G}_{h_c\eta^{(\prime)}}(q^2)|^2$ is shown. Schematically, we can clearly see that the modulus square $|f^{Q,G}_{h_c\eta^{(\prime)}}(q^2)|^2$ has only negligible changes in the range of (0–1000) MeV. Comparing the quark-antiquark contributions from $|f^{Q}_{h_c\eta^{(\prime)}}(q^2)|^2$ with the gluonic contributions from $|f^{G}_{h_c\eta^{(\prime)}}(q^2)|^2$, we find that the former is about twice that of the latter. In other words, the gluonic contributions and the quark-antiquark contributions are both important in these decay processes. It is compatible with the situation in the corresponding radiative decays $h_c \to \gamma\eta^{(\prime)}$ [51,52].

Based on the foregoing discussions, in the large-recoil-momentum region of $\eta^{(\prime)}$, the $h_c \to \eta^{(\prime)}\gamma^*$ TFFs can be obtained by

$$f^{H}_{h_c\eta^{(\prime)}}(q^2) = f^{Q}_{h_c\eta^{(\prime)}}(q^2) + f^{G}_{h_c\eta^{(\prime)}}(q^2), \tag{2.28}$$

which includes the dynamical structure information from the quark-antiquark content and the gluonic content of $\eta^{(\prime)}$. In addition, the relativistic corrections related to the internal momentum of h_c are taken into account in the TFFs. Specifically, there exist the kinematical corrections from the annihilation amplitudes and the dynamical corrections from the bound-state wave function of h_c. Since the physical picture in the large-recoil-momentum region of the electromagnetic Dalitz decays $h_c \to \eta^{(\prime)}\ell^+\ell^-$ is the same as the one in the corresponding radiative decays, these electromagnetic Dalitz decays can be calculated by the nonrelativistic quark model with the zero-binding approximation, as well as the Bethe-Salpeter formalism. Similarly to the situations in the radiative decays $h_c \to \eta^{(\prime)}\gamma$ [51,52], we find that these relativistic corrections also play an important role in the decay processes $h_c \to \eta^{(\prime)}\ell^+\ell^-$. Numerically, there is about a 2-times enhancement of $|f^{H}_{h_c\eta^{(\prime)}}(q^2)|^2$ over the results with the zero-binding approximation.

B. Soft mechanism

Generally speaking, a perturbative QCD approach will become invalid in the three-body decay processes $h_c \to \eta^{(\prime)}\ell^+\ell^-$ with a small recoil momentum of $\eta^{(\prime)}$, and a special handling is needed in principle. To deal with this issue properly, a picture of the soft wave function overlap is proposed in Ref. [15], where the picture has been proved valid in the decays $J/\psi \to \eta e^+e^-$ with a small recoil momentum. Because of the similar physical picture, the

TFFs of the $h_c \to \eta^{(\prime)}\gamma^*$ in the small-recoil-momentum region, which are dependent on the recoil momentum $|\mathbf{p}_{\eta^{(\prime)}}|$ and reflect the size effects from the spatial wave functions of the initial- and final-state hadrons, can be adopted in the empirical form in the rest frame of h_c [53,57,60,94]:

$$f^S_{h_c\eta^{(\prime)}}(q^2) = g_{h_c\eta^{(\prime)}} \exp\left(-\frac{\mathbf{q}^2}{8\beta^2}\right). \tag{2.29}$$

Here, $\boldsymbol{q}^2 = |\mathbf{p}_{\eta^{(\prime)}}|^2 = \lambda(M^2, m^2, q^2)/(4M^2)$, $g_{h_c\eta^{(\prime)}}$ denotes the $h_c - \eta^{(\prime)}$-γ^* coupling and can be determined by the continuity condition of the TFFs between the large- and the small-recoil-momentum regions, and the parameter β is an experiment-related quantity. We adopt $\beta = 400$ MeV, which is compatible with the fitted value in the J/ψ decays [15]. And it is worth noting that the decay amplitude $\mathcal{A}^{\alpha\beta}$ in soft mechanism has the form $ef^S_{h_c\eta^{(\prime)}}(q^2) \times (g^{\alpha\beta} - q^\alpha K^\beta/q\cdot K)$, in which the spin structure is determined just by the quantum number of the initial- and final-state hadrons.

In the whole recoil-momentum region of $\eta^{(\prime)}$, the TFFs can be given by

$$f_{h_c\eta^{(\prime)}}(q^2) = \begin{cases} f^H_{h_c\eta^{(\prime)}}(q^2) & q^2 \le 1\ \text{GeV}^2, \\ f^S_{h_c\eta^{(\prime)}}(q^2) & q^2 > 1\ \text{GeV}^2. \end{cases} \tag{2.30}$$

Incidentally, the recoil momentum $|\mathbf{p}_{\eta^{(\prime)}}| = \lambda^{\frac{1}{2}}(M^2, m^2, q^2)/(2M)$ is a monotonically decreasing function of the square of the invariant mass of the lepton pair q^2. The recoil momentum is above 1 GeV when $q^2 \le 1\ \text{GeV}^2$. It is commonly asserted that perturbative QCD is self-consistent when the recoil momentum is above 1 GeV [95–98]. Namely, the transition to perturbative QCD appears at about $q^2 = 1\ \text{GeV}^2$, and the hard mechanism begins to dominate as q^2 decreases. On the contrary, the contributions from the soft mechanism would become important with the increase of q^2. Although we could obtain the hard contributions from the large-recoil-momentum region with the perturbative QCD approach and the soft ones from the small-recoil-momentum region with the overlapping integration of the soft wave functions, how to precisely match these two contributions in the intermediate-recoil-momentum region is still an open question and needs further investigation. Even so, our description of the EM Dalitz decay processes $h_c \to \eta^{(\prime)}\ell^+\ell^-$ may constitute an important step forward toward a satisfactory description.

III. RESULTS AND DISCUSSIONS

In the rest frame of h_c, the q^2-dependent differential decay widths of $h_c \to \eta^{(\prime)}\ell^+\ell^-$ can be written as

$$\begin{aligned}\frac{\mathrm{d}\Gamma(h_c \to \eta^{(\prime)}\ell^+\ell^-)}{\mathrm{d}q^2} &= \frac{\alpha^2}{18\pi}\frac{\lambda^{\frac{1}{2}}(M^2, m^2, q^2)}{M^3}\frac{|f_{h_c\eta^{(\prime)}}(q^2)|^2}{q^2}\left(1+\frac{2m_\ell^2}{q^2}\right) \\ &\times \left(1-\frac{4m_\ell^2}{q^2}\right)^{\frac{1}{2}}\left(1+\frac{2M^2q^2}{(M^2-m^2+q^2)^2}\right),\end{aligned} \tag{3.1}$$

where m_ℓ is the lepton mass. In order to remove most of the uncertainties from the TFFs (a brief discussion in what follows), we relate the differential decay widths $\mathrm{d}\Gamma(h_c \to \eta^{(\prime)}\ell^+\ell^-)$ to the corresponding radiative decay widths $\Gamma(h_c \to \eta^{(\prime)}\gamma)$:

$$\begin{aligned}\frac{\mathrm{d}\Gamma(h_c \to \eta^{(\prime)}\ell^+\ell^-)}{\mathrm{d}q^2\Gamma(h_c \to \eta^{(\prime)}\gamma)} &= \frac{\alpha}{3\pi}|F_{h_c\eta^{(\prime)}}(q^2)|^2\frac{1}{q^2}\frac{\lambda^{\frac{1}{2}}(M^2, m^2, q^2)}{(M^2-m^2)} \\ &\times \left(1+\frac{2m_\ell^2}{q^2}\right)\left(1-\frac{4m_\ell^2}{q^2}\right)^{\frac{1}{2}} \\ &\times \left(1+\frac{2M^2q^2}{(M^2-m^2+q^2)^2}\right),\end{aligned} \tag{3.2}$$

where $F_{h_c\eta^{(\prime)}}(q^2) \equiv f_{h_c\eta^{(\prime)}}(q^2)/f_{h_c\eta^{(\prime)}}(0)$ are the normalized TFFs, and the normalization is such that $F_{h_c\eta^{(\prime)}}(0) = 1$.

In the numerical calculations, all the values of the involved meson masses, quark masses, decay widths and decay constant are quoted from the Particle Data Group [99]. By employing the two-loop renormalization group equation, we obtain the strong coupling constant $\alpha_s(m_c) = 0.38$. The effective mass of the c quark and the harmonic oscillator parameter appearing in the bound-state wave function are taken as $\hat{m}_c = 1490$ MeV and $\beta_A = 590$ MeV, respectively, and more discussions can be found in Refs. [100–102]. For the Gegenbauer moments from $\eta^{(\prime)}$ DAs, we just adopt model I in Table 1 of Ref. [52] due to the negligibly small uncertainties from these Gegenbauer moments, which have been mentioned in the foregoing discussions. For the phenomenological parameters—i.e., the mixing angle ϕ and the decay constants $f_{q(s)}$—we adopt the set of values [82]

$$\begin{aligned}&\phi = 33.5^\circ \pm 0.9^\circ, \qquad f_q = (1.09 \pm 0.02) f_\pi, \\ &f_s = (0.96 \pm 0.04) f_\pi\end{aligned} \tag{3.3}$$

extracted from the TFF $F_{\gamma^*\gamma\eta'}(+\infty)$, which is in excellent agreement with the *BABAR* measurement [103]. More discussions about these phenomenological parameters can be found in Refs. [11,51,52,76,80,104].

We now proceed with a full calculation of the branching ratios $\mathcal{B}(h_c \to \eta^{(\prime)}\ell^+\ell^-)$, and our numerical results are shown in Table I. Here, we do not present the theoretical uncertainties, which come mainly from $\mathcal{B}^{\exp}(h_c \to \eta\gamma) = (4.7 \pm 2.1) \times 10^{-4}$ or $\mathcal{B}^{\exp}(h_c \to \eta'\gamma) = (1.5 \pm 0.4) \times 10^{-3}$ [33], and they are expected to be $30\% \sim 50\%$.

TABLE I. The branching ratios $\mathcal{B}(h_c \to \eta^{(\prime)}\ell^+\ell^-)$.

	Hard mechanism	Soft mechanism	Total
$\mathcal{B}(h_c \to \eta e^+e^-)$	4.9×10^{-6}	3.7×10^{-6}	8.5×10^{-6}
$\mathcal{B}(h_c \to \eta \mu^+\mu^-)$	1.0×10^{-6}	3.7×10^{-6}	4.6×10^{-6}
$\mathcal{B}(h_c \to \eta' e^+e^-)$	1.6×10^{-5}	0.7×10^{-5}	2.3×10^{-5}
$\mathcal{B}(h_c \to \eta' \mu^+\mu^-)$	0.3×10^{-5}	0.7×10^{-5}	1.0×10^{-5}

In the second column, the results from the hard mechanism, which can be described by the perturbative QCD approach, are presented; in the third column, we show the results from the soft mechanism, which is governed by the overlapping integration of the wave functions of the initial- and final-state hadrons. The total contributions from both the hard mechanism and the soft mechanism are presented in the last column. First of all, it is noticed that the soft contributions in the decay processes $h_c \to \eta^{(\prime)}e^+e^-$ are equal to those in the decay processes $h_c \to \eta^{(\prime)}\mu^+\mu^-$ with an accuracy of more than three (two) significant digits. This is because the differential branching ratios are proportional to $(1 - \mathcal{O}(m_\ell^4/q^4))$ in the large-q^2 region [see Eqs. (3.1) or (3.2)]. Therefore, the difference caused by the lepton mass m_ℓ is ignorable in the small-recoil-momentum region. At the same time, the hard contributions of the $\mu^+\mu^-$ channel are about 5 times smaller than those of the e^+e^- channel, since the phase space of the former shrinks in the small-q^2 region. Besides this, we find that the hard contributions and the soft ones are comparable with each other. It is unlike the situation where the soft contributions are negligibly small in the S-wave charmonium EM Dalitz decays $J/\psi \to \eta^{(\prime)}\ell^+\ell^-$, because of a suppression of the kinematic factor (i.e., $|\mathbf{p}_{\eta^{(\prime)}}|^3/q$) [15]. It is worthwhile to point out that there are around 3×10^9 $\psi(2S)$ events collected with the BESIII detector so far [39–41], and this may imply that our predictions of the branching ratios $\mathcal{B}(h_c \to \eta^{(\prime)}\ell^+\ell^-)$ may come within the range of measurement of present or near-future experiments, especially for the η' channels (reaching 10^{-5}).

Last but not least, we concentrate on the q^2-dependent TFFs $f_{h_c\eta^{(\prime)}}(q^2)$, which could provide the dynamical information of the EM structure arising at the $h_c \to \eta^{(\prime)}$ transition vertex and offer a powerful probe of the intrinsic structure of the P-wave charmonium h_c. Experimentally, one is interested in the normalized TFFs $F_{h_c\eta^{(\prime)}}(q^2)$, because their modulus square $|F_{h_c\eta^{(\prime)}}(q^2)|^2$ can be directly extracted by comparing the measured invariant mass spectrum of the lepton pairs from the Dalitz decays with the pointlike QED prediction [10,62]. On the other hand, there exists a large uncertainty from sources such as the bound-state wave function and the QCD running coupling constant α_s in the TFFs $f_{h_c\eta^{(\prime)}}(q^2)$. However, the dependence of the normalized TFFs $F_{h_c\eta^{(\prime)}}(q^2)$ [i.e., the ratios $f_{h_c\eta^{(\prime)}}(q^2)/f_{h_c\eta^{(\prime)}}(0)$] on the bound-state wave function and the QCD running coupling constant is cut down to a large extent. So, one can expect that the predictions of the normalized TFFs are more reliable. Besides, the q^2 dependence of the TFFs $f_{h_c\eta^{(\prime)}}(q^2)$ is still retained in the normalized TFFs $F_{h_c\eta^{(\prime)}}(q^2)$ because of the constants $f_{h_c\eta^{(\prime)}}(0)$. In Fig. 4, we present the q^2 dependence of the modulus square of the normalized TFFs $|F_{h_c\eta^{(\prime)}}(q^2)|^2$ in their full kinematic region. Here it should be noted that, even though the normalized TFFs $|F_{h_c\eta^{(\prime)}}(q^2)|^2$ are independent of the lepton mass, the kinematic region of the e^+e^- channel is different from that of the $\mu^+\mu^-$ channel. Specifically, the value of the dilepton invariant mass $m_{\ell^+\ell^-}$ starts at $2m_e$ in the e^+e^- channel, and it starts at $2m_\mu$ in the $\mu^+\mu^-$ channel. As shown schematically in Fig. 4, the difference in the modulus squares $|F_{h_c\eta}(q^2)|^2$ and $|F_{h_c\eta'}(q^2)|^2$ mainly arise from their phase space. One can find that the modulus square $|F_{h_c\eta^{(\prime)}}(q^2)|^2$ is quite steady in the small-q^2 region and increasing rapidly in the large-q^2 region, which is compatible with the situation in the EM Dalitz decay processes $J\psi \to \eta^{(\prime)}\ell^+\ell^-$ [1,15]. Present or near-future experimental measurement is expected to provide tests for these predictions.

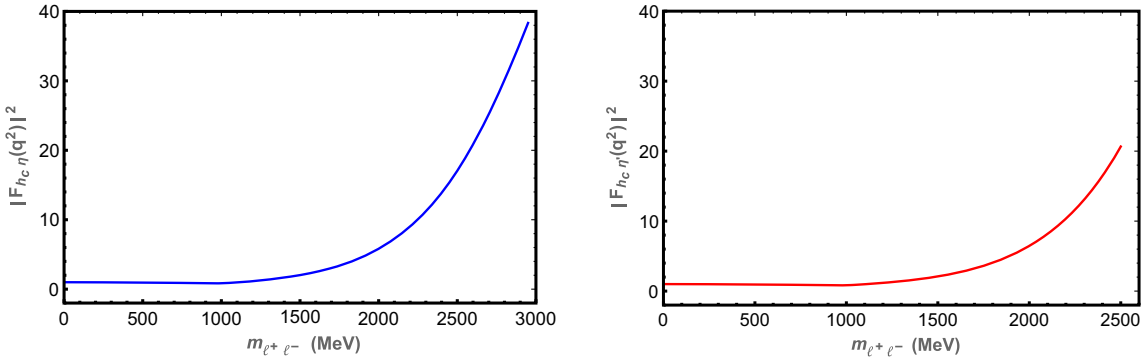

FIG. 4. The dependence of the modulus square of the normalized TFFs $|F_{h_c\eta^{(\prime)}}(q^2)|^2$ on the dilepton invariant mass $m_{\ell^+\ell^-}$ (or q^2).

IV. SUMMARY

In this paper, we investigate the P-wave charmonium EM Dalitz decays $h_c \to \eta^{(\prime)}\ell^+\ell^-$ with a QCD analysis. In the large-recoil-momentum region of $\eta^{(\prime)}$, these decay processes are described by the perturbative QCD approach. For the primary heavy meson h_c, we work out its B-S wave function in the framework of the B-S equation, and its internal momentum is retained in both the wave function and the hard-scattering amplitude; for the final light mesons $\eta^{(\prime)}$, the light-cone DAs are adopted due to a large momentum transfer. By an analytic calculation of the involved one-loop integrals, we find that the TFFs are UV and IR safe, and the gluonic contributions and the quark-antiquark contributions are both important in the TFFs. In the small-recoil-momentum region of $\eta^{(\prime)}$, the picture of the soft wave function overlap is adopted to describe the transition mechanism of $h_c \to \eta^{(\prime)}$. By relating to their radiative decay processes, the branching ratios $\mathcal{B}(h_c \to \eta^{(\prime)}\ell^+\ell^-)$ are obtained. Intriguingly, the contributions from the soft mechanism and those from the hard mechanism are comparable with each other, unlike the situation in S-wave charmonium decays $J/\psi \to \eta^{(\prime)}\ell^+\ell^-$ [15], where the soft contributions are suppressed because of the special form of the spin structure of their amplitudes. Furthermore, the q^2-dependent TFFs are analyzed briefly, and we obtain the q^2 dependence of the modulus square of the normalized TFFs $|F_{h_c\eta^{(\prime)}}(q^2)|^2$ in their full kinematic region. Lastly, it should be pointed out that there are around 3×10^9 $\psi(2S)$ events collected with the BESIII detector so far [39–41], and this may imply that our predictions of the branching ratios $\mathcal{B}(h_c \to \eta^{(\prime)}\ell^+\ell^-)$ may come within the range of measurement of present or near-future experiments, especially for the η' channels.

ACKNOWLEDGMENTS

This work is supported by the Guiding Project of Science and Technology Research Program of the Hubei Provincial Department of Education (Grant No. B2022160).

APPENDIX: THE EXPRESSIONS OF THE NINE NUMERATORS

The expressions of the numerators N_i $(i = 1 \sim 9)$ read

$$
\begin{aligned}
N_1 = {} & \frac{8if(\hat{k}^2)}{(M^4+m^4+q^4-2m^2(M^2+q^2)+4M^2q^2)}\frac{(M^2-m^2+q^2)}{(M^2-2m^2-2q^2+4m_c^2-8\hat{k}\cdot p-4\hat{k}^2)} \\
& \times \frac{1}{\hat{m}_c M}[2(2k_1^2(\hat{k}^2(m_c+\hat{m}_c)((m^2-q^2)^2-M^4)+2M^2\hat{k}\cdot p(2\hat{k}\cdot p(m_c-\hat{m}_c)-\hat{m}_c(m^2+2Mm_c+q^2))) \\
& + k_1\cdot p(4k_1\cdot q(\hat{k}^2(m_c+\hat{m}_c)(M^2-m^2+q^2)+\hat{m}_c\hat{k}\cdot p(2Mm_c-m^2+q^2)) \\
& + \hat{m}_c(m^2-M^2-q^2)(\hat{k}\cdot p(4\hat{k}^2+4\hat{k}\cdot p+3m^2-2M^2-4m_c^2+q^2)+2\hat{k}^2(m^2-M^2+q^2))) \\
& + \hat{m}_c k_1\cdot q(m^2-M^2-q^2)(\hat{k}\cdot p(4\hat{k}^2+4\hat{k}\cdot p+3m^2-4m_c^2+q^2)+4\hat{k}^2m^2)+(k_1\cdot p)^2(4\hat{k}^2(m_c+\hat{m}_c) \\
& \times (M^2-m^2+q^2)+4\hat{m}_c\hat{k}\cdot p(q^2+2M(M+m_c)-m^2)))-k_1\cdot\hat{k}(\hat{m}_c(m^2-M^2-q^2)(4\hat{k}^2(m^2+M^2-q^2) \\
& + 4\hat{k}\cdot p(m^2+M^2-q^2)+3m^4-m^2(M^2+4m_c^2+2q^2)+(M^2-q^2)(q-2m_c)(2m_c+q)) \\
& - 4k_1\cdot p(4M^2\hat{k}\cdot p(\hat{m}_c-m_c)+\hat{m}_c(m^2-M^2-q^2)(m^2-2Mm_c-q^2)))],
\end{aligned}
$$

$$
\begin{aligned}
N_2 = {} & \frac{8if(\hat{k}^2)}{(M^4+m^4+q^4-2m^2(M^2+q^2)+4M^2q^2)}\frac{(M^2-m^2+q^2)}{(M^2-2m^2-2q^2+4m_c^2+8\hat{k}\cdot p-4\hat{k}^2)} \\
& \times \frac{1}{\hat{m}_c M}[2(2k_1^2(\hat{k}^2(m_c+\hat{m}_c)(m^4-2m^2q^2-M^4+q^4)+2M^2\hat{m}_c\hat{k}\cdot p(m^2+2Mm_c+q^2) \\
& + 4M^2(\hat{k}\cdot p)^2(m_c-\hat{m}_c))+\hat{m}_c k_1\cdot q(m^2-M^2-q^2)(-\hat{k}\cdot p(4\hat{k}^2+3m^2-4m_c^2+q^2) \\
& + 4\hat{k}^2m^2+4(\hat{k}\cdot p)^2)+k_1\cdot p(\hat{m}_c(m^2-M^2-q^2)(-\hat{k}\cdot p(4\hat{k}^2+3m^2-2M^2-4m_c^2+q^2) \\
& + 2\hat{k}^2(m^2-M^2+q^2)+4(\hat{k}\cdot p)^2)-4k_1\cdot q(\hat{k}^2(m_c+\hat{m}_c)(m^2-M^2-q^2) \\
& + \hat{m}_c\hat{k}\cdot p(2Mm_c-m^2+q^2)))-4(k_1\cdot p)^2(\hat{k}^2(m_c+\hat{m}_c)(m^2-M^2-q^2)+\hat{m}_c\hat{k}\cdot p \\
& \times (2M^2-m^2+2Mm_c+q^2)))+k_1\cdot\hat{k}(\hat{m}_c(m^2-M^2-q^2)(4\hat{k}^2(m^2+M^2-q^2) \\
& - 4\hat{k}\cdot p(m^2+M^2-q^2)+3m^4-m^2M^2-4m^2m_c^2-2m^2q^2-4M^2m_c^2+M^2q^2+4m_c^2q^2-q^4) \\
& - 4k_1\cdot p(4M^2\hat{k}\cdot p(m_c-\hat{m}_c)+\hat{m}_c(m^2-M^2-q^2)(m^2-2Mm_c-q^2)))],
\end{aligned}
$$

$$
\begin{aligned}
N_3 = & \frac{8if(\hat{k}^2)}{(M^4+m^4+q^4-2m^2(M^2+q^2)+4M^2q^2)}\frac{(M^2-m^2+q^2)}{(M^2-2m^2-2q^2+4m_c^2-8\hat{k}\cdot p-4\hat{k}^2)} \\
& \times \frac{1}{\hat{m}_c M}[4k_1^2\hat{k}^2(m_c+\hat{m}_c)((m^2-q^2)^2-M^4)+2\hat{m}_c\hat{k}\cdot p(k_1\cdot q(4\hat{k}^2(M^2-m^2+q^2) \\
& +m^4+m^2(3M^2-8Mm_c+4m_c^2-2q^2)-(M^2+q^2)(4m_c^2-q^2))-4k_1^2M^2(m^2+2Mm_c+q^2)) \\
& +8(\hat{k}\cdot p)^2(2k_1^2M^2(m_c-\hat{m}_c)+\hat{m}_c k_1\cdot q(M^2-m^2+q^2))+2k_1\cdot p(\hat{m}_c\hat{k}\cdot p \\
& \times(4k_1\cdot q(2Mm_c-m^2+q^2)+q^2(4\hat{k}^2-2m^2+3M^2-4m_c^2)+(m^2-M^2)(-4\hat{k}^2+m^2 \\
& +2M^2-8Mm_c+4m_c^2)+q^4)+2\hat{k}^2(m^2-M^2-q^2)(m_c(m^2-M^2+q^2)-2k_1\cdot q(m_c \\
& +\hat{m}_c))+4(\hat{k}\cdot p)^2(\hat{m}_c(q^2-m^2)+M^2(3\hat{m}_c-2m_c)))+8(k_1\cdot p)^2(\hat{k}^2(m_c+\hat{m}_c) \\
& \times(M^2-m^2+q^2)+\hat{m}_c\hat{k}\cdot p(-m^2+2M(M+m_c)+q^2))+8\hat{k}^2m^2m_c k_1\cdot q(m^2-M^2-q^2) \\
& +k_1\cdot\hat{k}(4\hat{k}\cdot p(4M^2k_1\cdot p(\hat{m}_c-m_c)+m^4\hat{m}_c+m^2(4M^2(m_c-\hat{m}_c)-2\hat{m}_c q^2)+\hat{m}_c \\
& \times(q^4-M^4))-\hat{m}_c(m^2-M^2-q^2)(4k_1\cdot p(2Mm_c-m^2+q^2)-4\hat{k}^2(m^2+M^2-q^2) \\
& +m^4+m^2(M^2-8Mm_c+4m_c^2-2q^2)-(M^2-q^2)(q^2-2m_c^2)))],
\end{aligned}
$$

$$
\begin{aligned}
N_4 = & \frac{8if(\hat{k}^2)}{(M^4+m^4+q^4-2m^2(M^2+q^2)+4M^2q^2)}\frac{(M^2-m^2+q^2)}{(M^2-2m^2-2q^2+4m_c^2+8\hat{k}\cdot p-4\hat{k}^2)} \\
& \times \frac{1}{\hat{m}_c M}[4k_1^2\hat{k}^2(m_c+\hat{m}_c)((m^2-q^2)^2-M^4)+2\hat{m}_c\hat{k}\cdot p(4k_1^2M^2(m^2+2Mm_c+q^2) \\
& -k_1\cdot q(4\hat{k}^2(M^2-m^2+q^2)+m^4+m^2(3M^2-8Mm_c+4m_c^2-2q^2)-(M^2+q^2) \\
& \times(4m_c^2-q^2)))+8(\hat{k}\cdot p)^2(2k_1^2M^2(m_c-\hat{m}_c)+\hat{m}_c k_1\cdot q(M^2-m^2+q^2))+2k_1\cdot p \\
& \times(\hat{m}_c\hat{k}\cdot p(4k_1\cdot q(m^2-2Mm_c-q^2)+q^2(-4\hat{k}^2+2m^2-3M^2+4m_c^2)-(m^2-M^2) \\
& \times(-4\hat{k}^2+m^2+2M^2-8Mm_c+4m_c^2)-q^4)+2\hat{k}^2(m^2-M^2-q^2)(m_c(m^2-M^2+q^2) \\
& -2k_1\cdot q(m_c+\hat{m}_c))+4(\hat{k}\cdot p)^2(\hat{m}_c(q^2-m^2)+M^2(3\hat{m}_c-2m_c)))+8(k_1\cdot p)^2(\hat{k}^2 \\
& \times(m_c+\hat{m}_c)(M^2-m^2+q^2)+\hat{m}_c\hat{k}\cdot p(m^2-2M(M+m_c)-q^2))+8\hat{k}^2m^2m_c k_1\cdot q \\
& \times(m^2-M^2-q^2)+k_1\cdot\hat{k}(\hat{m}_c(m^2-M^2-q^2)(4k_1\cdot p(2Mm_c-m^2+q^2)-4\hat{k}^2(m^2 \\
& +M^2-q^2)+m^4+m^2(M^2-8Mm_c+4m_c^2-2q^2)-(M^2-q^2)(q^2-4m_c^2))+4\hat{k}\cdot p \\
& \times(4M^2k_1\cdot p(\hat{m}_c-m_c)+m^4\hat{m}_c+m^2(4M^2(m_c-\hat{m}_c)-2\hat{m}_c q^2)+\hat{m}_c(q^4-M^4)))],
\end{aligned}
$$

$$
\begin{aligned}
N_5 = & \frac{2if(\hat{k}^2)}{(M^4+m^4+q^4-2m^2(M^2+q^2)+4M^2q^2)}\frac{(M^2-m^2+q^2)}{(M^2-2m^2-2q^2+4m_c^2-8\hat{k}\cdot p-4\hat{k}^2)} \\
& \times \frac{1}{\hat{m}_c M}[-8k_1^2\hat{k}^2\hat{m}_c((m^2-q^2)^2-M^4)+k_1\cdot\hat{k}((m^2-M^2-q^2)(\hat{m}_c(-4k_1^2(m^2+M^2-q^2)+m^4 \\
& +m^2(M^2-4Mm_c-4m_c^2-2q^2)+(M^2-q^2)(4m_c(M-m_c)-q^2)) \\
& +4\hat{k}^2(2m_c-\hat{m}_c)(m^2+M^2-q^2))-4\hat{k}\cdot p(4(k_1\cdot p+k_1\cdot q)(m^2(2m_c-\hat{m}_c)-M^2\hat{m}_c \\
& +q^2(\hat{m}_c-2m_c))+(m^2+M^2-q^2)(\hat{m}_c(m^2-q^2)+M^2(\hat{m}_c-2m_c)))-8\hat{m}_c \\
& \times(m^2-2k_1\cdot p)(k_1\cdot p+k_1\cdot q)(m^2-M^2-q^2))-2\hat{k}\cdot p(k_1\cdot p(\hat{m}_c(-4k_1^2(m^2+3M^2-q^2) \\
& +q^2(-2m^2+3M^2-4Mm_c+4m_c^2)+(m-M)(m+M)(m^2+2M^2-4Mm_c-4m_c^2)+q^4) \\
& +16\hat{m}_c k_1\cdot q(k_1\cdot q-m^2)+4\hat{k}^2(2m_c-\hat{m}_c)(m^2-M^2-q^2))+k_1\cdot q \\
& \times(\hat{m}_c(-4k_1^2(m^2+3M^2-q^2)+m^4+m^2((M-2m_c)(3M+2m_c)-2q^2)-(M^2+q^2)
\end{aligned}
$$

$$\times (4m_c(M-m_c)-q^2))-8m^2\hat{m}_c k_1\cdot q+4\hat{k}^2(2m_c-\hat{m}_c)(m^2-M^2-q^2))+4k_1^2M^2$$
$$\times \hat{m}_c(m^2+M^2-q^2)-8\hat{m}_c(k_1\cdot p)^2(m^2-4k_1\cdot q)+16\hat{m}_c(k_1\cdot p)^3)-4\hat{k}^2\hat{m}_c(m^2-M^2-q^2)$$
$$\times (k_1\cdot p(-4k_1\cdot p+m^2-M^2+q^2)+2k_1\cdot q(m^2-2k_1\cdot p))+8m_c(k_1\cdot\hat{k})^2((m^2-q^2)^2-M^4)$$
$$+8(\hat{k}\cdot p)^2(k_1\cdot p+k_1\cdot q)(4(m_c-\hat{m}_c)(k_1\cdot p+k_1\cdot q)+\hat{m}_c(m^2-q^2)+M^2(\hat{m}_c-2m_c))],$$

$$N_6=\frac{2i(M^2-m^2+q^2)f(\hat{k}^2)}{\hat{m}_c M(M^4+m^4+q^4-2m^2(M^2+q^2)+4M^2q^2)}[-8k_1^2\hat{k}^2\hat{m}_c((m^2-q^2)^2-M^4)$$
$$+k_1\cdot\hat{k}(-(m^2-M^2-q^2)(\hat{m}_c(-4k_1^2(m^2+M^2-q^2)+m^4+m^2(M^2-4Mm_c-4m_c^2-2q^2)$$
$$+(M^2-q^2)(4m_c(M-m_c)-q^2))+4\hat{k}^2(2m_c-\hat{m}_c)(m^2+M^2-q^2))-4\hat{k}\cdot p$$
$$\times (4(k_1\cdot p+k_1\cdot q)(m^2(2m_c-\hat{m}_c)-M^2\hat{m}_c+q^2(\hat{m}_c-2m_c))+(m^2+M^2-q^2)$$
$$\times (\hat{m}_c(m^2-q^2)+M^2(\hat{m}_c-2m_c)))+8\hat{m}_c(m^2-2k_1\cdot p)(k_1\cdot p+k_1\cdot q)(m^2-M^2-q^2))$$
$$+2\hat{k}\cdot p(k_1\cdot p(\hat{m}_c(-4k_1^2(m^2+3M^2-q^2)+q^2(3M^2-2m^2-4Mm_c+4m_c^2)$$
$$+(m^2-M^2)(m^2+2M^2-4Mm_c-4m_c^2)+q^4)+16\hat{m}_c k_1\cdot q(k_1\cdot q-m^2)+4\hat{k}^2(2m_c-\hat{m}_c)$$
$$\times (m^2-M^2-q^2))+k_1\cdot q(\hat{m}_c(-4k_1^2(m^2+3M^2-q^2)+m^4+m^2((M-2m_c)$$
$$\times (3M+2m_c)-2q^2)-(M^2+q^2)(4m_c(M-m_c)-q^2))-8m^2\hat{m}_c k_1\cdot q+4\hat{k}^2(2m_c-\hat{m}_c)$$
$$\times (m^2-M^2-q^2))+4k_1^2M^2\hat{m}_c(m^2+M^2-q^2)-8\hat{m}_c(k_1\cdot p)^2(m^2-4k_1\cdot q)$$
$$+16\hat{m}_c(k_1\cdot p)^3)-4\hat{k}^2\hat{m}_c(m^2-M^2-q^2)(k_1\cdot p(-4k_1\cdot p+m^2-M^2+q^2)+2k_1\cdot q$$
$$\times (m^2-2k_1\cdot p))+8m_c(k_1\cdot\hat{k})^2((m^2-q^2)^2-M^4)+8(\hat{k}\cdot p)^2(k_1\cdot p+k_1\cdot q)$$
$$\times (4(m_c-\hat{m}_c)(k_1\cdot p+k_1\cdot q)+\hat{m}_c(m^2-q^2)+M^2(\hat{m}_c-2m_c))],$$

$$N_7=\frac{i(M^2-m^2+q^2)f(\hat{k}^2)}{2\hat{m}_c M(M^4+m^4+q^4-2m^2(M^2+q^2)+4M^2q^2)}\frac{1}{(M^2+m^2-q^2+\lambda^{\frac{1}{2}}(M^2,q^2,m^2))}$$
$$\times\frac{1}{\lambda^{\frac{1}{2}}(M^2,q^2,m^2)}[\lambda(M^2,q^2,m^2)(M^2(\hat{k}\cdot p)(4u(\hat{m}_c-m_c)(\hat{k}\cdot p)+\hat{m}_c(m^2(2u-1)$$
$$+M^2-4Mm_c u-2q^2u+q^2))-\hat{k}^2(m^4-2m^2q^2-M^4+q^4)(m_c u+\hat{m}_c(u-1)))$$
$$+\lambda^{\frac{1}{2}}(M^2,q^2,m^2)(M^2(\hat{k}\cdot p)(4(\hat{k}\cdot p)(m^2(\hat{m}_c(u-1)-m_c u)+M^2(-m_c u+\hat{m}_c u+\hat{m}_c)$$
$$+q^2(m_c u+\hat{m}_c(-u)+\hat{m}_c))+\hat{m}_c(-2m^4(u-1)+m^2(M^2(2u-3)+4Mm_c u-4m_c^2)$$
$$+M^4-4M^3m_c u+M^2(4m_c^2-q^2(2u+1))+4Mm_c q^2u+4m_c^2q^2+2q^4u-2q^4))-\hat{k}^2$$
$$\times (m^2-M^2-q^2)((m^4-2m^2(M^2+q^2)+(M^2-q^2)^2)(m_c u+\hat{m}_c(u-1))-4M^2\hat{m}_c$$
$$\times (\hat{k}\cdot p)))+M^2(\hat{k}\cdot p)(4\hat{m}_c\hat{k}^2(m^4-2m^2q^2-M^4+q^4)-4(\hat{k}\cdot p)(m^4\hat{m}_c-2m^2(\hat{m}_c$$
$$\times (2M^2u+q^2)-2M^2m_c u)+\hat{m}_c(q^4-M^4))-\hat{m}_c(m^2-M^2-q^2)(m^4(4u-3)$$
$$+m^2(M^2-8Mm_c u+4m_c^2+2q^2(1-2u))-(M^2-q^2)(q^2-4m_c^2)))],$$

$$N_8=\frac{i(M^2-m^2+q^2)f(\hat{k}^2)}{2\hat{m}_c M(M^4+m^4+q^4-2m^2(M^2+q^2)+4M^2q^2)}\frac{1}{(M^2+m^2-q^2+\lambda^{\frac{1}{2}}(M^2,q^2,m^2))}$$
$$\times\frac{1}{\lambda^{\frac{1}{2}}(M^2,q^2,m^2)}[\lambda^{\frac{1}{2}}(M^2,q^2,m^2)(M^2(\hat{k}\cdot p)(4(2u-1)(\hat{k}\cdot p)(\hat{m}_c(q^2-m^2)+M^2(2m_c-\hat{m}_c))$$
$$+\hat{m}_c(-m^2(M^2(1-2u)^2-4m_c^2+4q^2(u-1)u)+M^4(1-2u)^2-M^2(4m_c^2+q^2$$
$$\times (8u^2-8u+3))+8Mm_c q^2-4m_c^2q^2+4q^4(u-1)u))-\hat{k}^2(m^2-M^2-q^2)(4M^2(2m_c$$

$$
\begin{aligned}
&- \hat{m}_c)(\hat{k}\cdot p) + \hat{m}_c(2u-1)(m^4 - 2m^2(M^2+q^2) + (M^2-q^2)^2))) + \hat{m}_c\lambda(M^2,q^2,m^2)\\
&\times (M^2(\hat{k}\cdot p)(m^2(1-2u)^2 + M^2(1-2u)^2 - 4Mm_c - q^2(1-2u)^2) - (2u-1)\hat{k}^2(m^4\\
&- 2m^2q^2 - M^4 + q^4))) + M^2(\hat{k}\cdot p)(-4(2u-1)(m^2+M^2-q^2)(\hat{k}\cdot p)(\hat{m}_c(m^2-q^2)\\
&+ M^2(\hat{m}_c - 2m_c)) - 4\hat{k}^2(2m_c - \hat{m}_c)(m^4 - 2m^2q^2 - M^4 + q^4) - \hat{m}_c(m^2 - M^2 - q^2)\\
&\times (m^4(1-2u)^2 + m^2(M^2(1-2u)^2 - 4Mm_c - 4m_c^2 - 2q^2(2u^2-2u+1))\\
&+ (M^2-q^2)(4Mm_c - 4m_c^2 - q^2)))],
\end{aligned}
$$

$$
\begin{aligned}
N_9 = &\frac{i(M^2-m^2+q^2)f(\hat{k}^2)}{2\hat{m}_c M(M^4+m^4+q^4-2m^2(M^2+q^2)+4M^2q^2)}\frac{1}{(M^2+m^2-q^2+\lambda^{\frac{1}{2}}(M^2,q^2,m^2))}\\
&\times\frac{1}{\lambda^{\frac{1}{2}}(M^2,q^2,m^2)}[\lambda(M^2,q^2,m^2)(M^2(\hat{k}\cdot p)(\hat{m}_c(m^2(1-2u)+M^2+4Mm_c(u-1)\\
&+ q^2(2u-1)) - 4(u-1)(m_c-\hat{m}_c)(\hat{k}\cdot p)) - \hat{k}^2(m^4-2m^2q^2-M^4+q^4)(m_c(u-1)\\
&+ \hat{m}_c u)) - \lambda^{\frac{1}{2}}(M^2,q^2,m^2)(\hat{k}^2(m^2-M^2-q^2)((m^4-2m^2(M^2+q^2)+(M^2-q^2)^2)\\
&\times (m_c(u-1)+\hat{m}_c u) - 4M^2\hat{m}_c(\hat{k}\cdot p)) + M^2(\hat{k}\cdot p)(4(\hat{k}\cdot p)(m^2(m_c(u-1)-\hat{m}_c u)\\
&+ M^2(m_c(u-1)-\hat{m}_c(u-2)) + q^2(m_c(-u)+m_c+\hat{m}_c u)) + \hat{m}_c(-2m^4u + m^2(M^2\\
&\times (2u+1) + 4Mm_c(u-1) + 4m_c^2) - M^4 - 4M^3m_c(u-1) + M^2(q^2(3-2u) - 4m_c^2)\\
&+ 4Mm_cq^2(u-1) - 4m_c^2q^2 + 2q^4u))) + M^2(\hat{k}\cdot p)(4\hat{m}_c\hat{k}^2(m^4-2m^2q^2-M^4+q^4)\\
&+ 4(\hat{k}\cdot p)(m^4\hat{m}_c - 2m^2(2M^2(u-1)(m_c-\hat{m}_c)+\hat{m}_c q^2) + \hat{m}_c(q^4-M^4)) + \hat{m}_c(m^2\\
&- M^2 - q^2)(m^4(4u-1) - m^2(M^2 + 8Mm_c(u-1) + 4m_c^2 + 2q^2(2u-1))\\
&+ (M^2-q^2)(q^2-4m_c^2)))],
\end{aligned}
$$

with $\lambda(a,b,c) \equiv a^2+b^2+c^2-2(ab+bc+ac)$ as the usual Källén function.

[1] M. Ablikim *et al.* (BESIII Collaboration), Observation of electromagnetic Dalitz decays $J/\psi \to Pe^+e^-$, Phys. Rev. D **89**, 092008 (2014).

[2] M. Ablikim *et al.* (BESIII Collaboration), Observation of $\psi(3686) \to \eta' e^+e^-$, Phys. Lett. B **783**, 452 (2018).

[3] M. Ablikim *et al.* (BESIII Collaboration), Measurement of $\mathcal{B}(J/\psi \to \eta' e^+e^-)$ and search for a dark photon, Phys. Rev. D **99**, 012013 (2019).

[4] M. Ablikim *et al.* (BESIII Collaboration), Study of the Dalitz decay $J/\psi \to e^+e^-\eta$, Phys. Rev. D **99**, 012006 (2019); **104**, 099901(E) (2021).

[5] M. Ablikim *et al.* (BESIII Collaboration), Study of electromagnetic Dalitz decays $\chi_{cJ} \to \mu^+\mu^- J/\psi$, Phys. Rev. D **99**, 051101 (2019).

[6] M. Ablikim *et al.* (BESIII Collaboration), Search for rare decay $J/\psi \to \phi e^+e^-$, Phys. Rev. D **99**, 052010 (2019).

[7] M. Ablikim *et al.* (BESIII Collaboration), Observation of J/ψ electromagnetic Dalitz decays to $X(1835)$, $X(2120)$ and $X(2370)$, Phys. Rev. Lett. **129**, 022002 (2022).

[8] M. Ablikim *et al.* (BESIII Collaboration), Observation of the hindered electromagnetic Dalitz decay $\psi(3686) \to e^+e^-\eta_c$, Phys. Rev. D **106**, 112002 (2022).

[9] M. Ablikim *et al.* (BESIII Collaboration), Observation of the decay $J/\psi \to e^+e^-\eta(1405)$ with $\eta(1405) \to \pi^0 f_0(980)$, Phys. Rev. D **109**, 012007 (2024).

[10] J. Fu, H.-B. Li, X. Qin, and M.-Z. Yang, Study of the electromagnetic transitions $J/\psi \to Pl^+l^-$ and probe dark photon, Mod. Phys. Lett. A **27**, 1250223 (2012).

[11] Y.-H. Chen, Z.-H. Guo, and B.-S. Zou, Unified study of $J/\psi \to PV$, $P\gamma^{(*)}$ and light hadron radiative processes, Phys. Rev. D **91**, 014010 (2015).

[12] B. Kubis and F. Niecknig, Analysis of the $J/\psi \to \pi^0\gamma^*$ transition form factor, Phys. Rev. D **91**, 036004 (2015).

[13] L.-M. Gu, H.-B. Li, X.-X. Ma, and M.-Z. Yang, Study of the electromagnetic Dalitz decays $\psi(\Upsilon) \to \eta_c(\eta_b)l^+l^-$, Phys. Rev. D **100**, 016018 (2019).

[14] J. Zhang, J. He, T. Zhu, S. Xu, and R. Wang, Study of vector charmonium electromagnetic Dalitz decays, Int. J. Mod. Phys. A **34**, 1950129. (2019).

[15] J.-K. He and C.-J. Fan, QCD analysis of electromagnetic Dalitz decays $J/\psi \to \eta^{(\prime)}\ell^+\ell^-$, Phys. Rev. D **105**, 094034 (2022).

[16] L.-W. Yan, Y.-H. Chen, C.-G. Duan, and Z.-H. Guo, Effective-Lagrangian study of $\psi'(J/\psi) \to VP$ and the insights into the $\rho\pi$ puzzle, Phys. Rev. D **107**, 034022 (2023).

[17] L. G. Landsberg, Electromagnetic leptonic decays and structure of light mesons, Sov. Phys. Usp. **28**, 435 (1985).

[18] L. G. Landsberg, Electromagnetic decays of light mesons, Phys. Rep. **128**, 301 (1985).

[19] S. L. Adler, Axial vector vertex in spinor electrodynamics, Phys. Rev. **177**, 2426 (1969).

[20] J. S. Bell and R. Jackiw, A PCAC puzzle: $\pi^0 \to \gamma\gamma$ in the σ model, Nuovo Cimento A **60**, 47 (1969).

[21] S. Weinberg, The U(1) problem, Phys. Rev. D **11**, 3583 (1975).

[22] E. Witten, Instantons, the quark model, and the $1/n$ expansion, Nucl. Phys. **B149**, 285 (1979).

[23] E. Witten, Current algebra theorems for the U(1) Goldstone boson, Nucl. Phys. **B156**, 269 (1979).

[24] G. Veneziano, U(1) without instantons, Nucl. Phys. **B159**, 213 (1979).

[25] T. Feldmann, P. Kroll, and B. Stech, Mixing and decay constants of pseudoscalar mesons, Phys. Rev. D **58**, 114006 (1998).

[26] T. Feldmann, Quark structure of pseudoscalar mesons, Int. J. Mod. Phys. A **15**, 159 (2000).

[27] R. Escribano and E. Royo, π^0-η-η' mixing from $V \to P\gamma$ and $P \to V\gamma$ decays, Phys. Lett. B **807**, 135534 (2020).

[28] A. Kazi, G. Kramer, and D. H. Schiller, Decay of the $\psi(3.1)$ in broken SU_4, Lett. Nuovo Cimento **15**, 120 (1976).

[29] H. Fritzsch and J. D. Jackson, Mixing of pseudoscalar mesons and M1 radiative decays, Phys. Lett. **66B**, 365 (1977).

[30] N. M. Kroll and W. Wada, Internal pair production associated with the emission of high-energy gamma rays, Phys. Rev. **98**, 1355 (1955).

[31] M. Ablikim *et al.* (BESIII Collaboration), Measurements of $h_c(^1P_1)$ in ψ' decays, Phys. Rev. Lett. **104**, 132002 (2010).

[32] M. Ablikim *et al.* (BESIII Collaboration), Study of the $hc(1^1P_1)$ meson via $\psi(2S) \to \pi^0 h_c$ decays at BESIII, Phys. Rev. D **106**, 072007 (2022).

[33] M. Ablikim *et al.* (BESIII Collaboration), Observation of h_c radiative decay $h_c \to \gamma\eta'$ and evidence for $h_c \to \gamma\eta$, Phys. Rev. Lett. **116**, 251802 (2016).

[34] M. Ablikim *et al.* (BESIII Collaboration), Search for $h_c \to \pi^+\pi^- J/\psi$ via $\psi(3686) \to \pi^0\pi^+\pi^- J/\psi$, Phys. Rev. D **97**, 052008 (2018).

[35] M. Ablikim *et al.* (BESIII Collaboration), First observations of $h_c \to$ hadrons, Phys. Rev. D **99**, 072008 (2019).

[36] M. Ablikim *et al.* (BESIII Collaboration), Search for new hadronic decays of h_c and observation of $h_c \to K^+K^-\pi^+\pi^-\pi^0$, Phys. Rev. D **102**, 112007 (2020).

[37] M. Ablikim *et al.* (BESIII Collaboration), Search for the decay $h_c \to \pi^0 J/\psi$, J. High Energy Phys. 05 (2022) 003.

[38] M. Ablikim *et al.* (BESIII Collaboration), Search for new hadronic decays of h_c and observation of $h_c \to p\bar{p}\eta$, J. High Energy Phys. 05 (2022) 108; 03 (2023) 22.

[39] M. Ablikim *et al.* (BESIII Collaboration), Future physics programme of BESIII, Chin. Phys. C **44**, 040001 (2020).

[40] M. Ablikim (BESIII Collaboration), Observation of $\psi(3686) \to \Lambda\bar{\Lambda}\eta'$ decay, Phys. Rev. D **108**, 112014 (2023).

[41] M. Ablikim *et al.* (BESIII Collaboration), Updated measurements of the M1 transition $\psi(3686) \to \gamma\eta_c(2S)$ with $\eta_c(2S) \to K\bar{K}\pi$, Phys. Rev. D **109**, 032004 (2024).

[42] F. J. Gilman and R. Kauffman, The η-η' mixing angle, Phys. Rev. D **36**, 2761 (1987).

[43] P. Ball, J. M. Frère, and M. Tytgat, Phenomenological evidence for the gluon content of η and η', Phys. Lett. B **365**, 367 (1996).

[44] R. Barbieri, R. Gatto, and E. Remiddi, Singular binding dependence in the hadronic widths of 1^{++} and 1^{+-} heavy quark anti-quark bound states, Phys. Lett. **61B**, 465 (1976).

[45] R. Barbieri, M. Caffo, R. Gatto, and E. Remiddi, Strong QCD corrections to p wave quarkonium decays, Phys. Lett. **95B**, 93 (1980).

[46] R. Barbieri, M. Caffo, R. Gatto, and E. Remiddi, QCD corrections to p wave quarkonium decays, Nucl. Phys. **B192**, 61 (1981).

[47] P. Kroll, Exclusive charmonium decays, Nucl. Phys. B, Proc. Suppl. **64**, 456 (1998).

[48] S. M. H. Wong, Color octet contribution to exclusive P wave charmonium decay into nucleon-antinucleon, Nucl. Phys. B, Proc. Suppl. **74**, 231 (1999).

[49] S. M. H. Wong, Color octet contribution in exclusive P wave charmonium decay into proton-antiproton, Nucl. Phys. **A674**, 185 (2000).

[50] S. M. H. Wong, Color octet contribution in exclusive P wave charmonium decay, Nucl. Phys. B, Proc. Suppl. **93**, 220 (2001).

[51] J.-K. He and C.-J. Fan, Revisiting the P-wave charmonium radiative decays $h_c \to \gamma\eta^{(\prime)}$ with relativistic corrections, Phys. Rev. D **103**, 114006 (2021).

[52] C.-J. Fan and J.-K. He, Radiative decays of h_c to the light mesons $\eta^{(\prime)}$: A perturbative QCD calculation, Phys. Rev. D **100**, 034005 (2019).

[53] C. Amsler and F. E. Close, Is $f_0(1500)$ a scalar glueball? Phys. Rev. D **53**, 295 (1996).

[54] A. V. Radyushkin, Nonforward parton densities and soft mechanism for form-factors and wide angle Compton scattering in QCD, Phys. Rev. D **58**, 114008 (1998).

[55] A. V. Radyushkin, QCD sum rules and soft-hard interplay for hadronic form-factors, Few Body Syst. Suppl. **11**, 57 (1999).

[56] T. Feldmann and P. Kroll, Skewed parton distributions for $B \to \pi$ transitions, Eur. Phys. J. C **12**, 99 (2000).

[57] F. E. Close and A. Kirk, The mixing of the $f_0(1370)$, $f_0(1500)$ and $f_0(1710)$ and the search for the scalar glueball, Phys. Lett. B **483**, 345 (2000).

[58] H. W. Huang and P. Kroll, Large momentum transfer electroproduction of mesons, Eur. Phys. J. C **17**, 423 (2000).

[59] C.-H. Chang, Y.-Q. Chen, G.-L. Wang, and H.-S. Zong, Decays of the meson B_c to a P wave charmonium state χ_c or h_c, Phys. Rev. D **65**, 014017 (2001).
[60] G. Li, Q. Zhao, and C.-H. Chang, Decays of J/ψ and ψ' into vector and pseudoscalar meson and the pseudoscalar glueball-$q\bar{q}$ mixing, J. Phys. G **35**, 055002 (2008).
[61] Q. Zhao, Understanding the radiative decays of vector charmonia to light pseudoscalar mesons, Phys. Lett. B **697**, 52 (2011).
[62] L. G. Landsberg, Electromagnetic decays of light mesons, Phys. Rep. **128**, 301 (1985).
[63] G. W. Intemann, Radiative decays of heavy quarkonia in an extended vector dominance model, Phys. Rev. D **27**, 2755 (1983).
[64] E. E. Salpeter and H. A. Bethe, A relativistic equation for bound state problems, Phys. Rev. **84**, 1232 (1951).
[65] E. E. Salpeter, Mass corrections to the fine structure of hydrogen-like atoms, Phys. Rev. **87**, 328 (1952).
[66] A. N. Mitra and S. Bhatnagar, Hadron-quark vertex function. Interconnection between 3D and 4D wave function, Int. J. Mod. Phys. A **07**, 121 (1992).
[67] S. Bhatnagar, S.-Y. Li, and J. Mahecha, Power counting of various Dirac covariants in hadronic Bethe-Salpeter wave functions for decay constant calculations of pseudoscalar mesons, Int. J. Mod. Phys. E **20**, 1437 (2011).
[68] S. Bhatnagar, J. Mahecha, and Y. Mengesha, Relevance of various Dirac covariants in hadronic Bethe-Salpeter wave functions in electromagnetic decays of ground state vector mesons, Phys. Rev. D **90**, 014034 (2014).
[69] B. Guberina, J. H. Kühn, R. D. Peccei, and R. Rückl, Rare decays of the Z^0, Nucl. Phys. **B174**, 317 (1980).
[70] B. Guberina and J. H. Kühn, Complete evaluation of $\Upsilon \to \gamma\eta_c$ in the quarkonium model, Lett. Nuovo Cimento **32**, 295 (1981).
[71] J. G. Körner, J. H. Kühn, M. Krammer, and H. Schneider, Zweig forbidden radiative orthoquarkonium decays in perturbative QCD, Nucl. Phys. **B229**, 115 (1983).
[72] K.-T. Chao, H.-W. Huang, and Y.-Q. Liu, Gluonic and leptonic decays of heavy quarkonia and the determination of $\alpha_s(m_c)$ and $\alpha_s(m_b)$, Phys. Rev. D **53**, 221 (1996).
[73] T. Muta and M.-Z. Yang, $\eta' - g^* - g$ transition form factor with gluon content contribution tested, Phys. Rev. D **61**, 054007 (2000).
[74] M.-Z. Yang and Y.-D. Yang, Revisiting charmless two-body B decays involving η' and η, Nucl. Phys. **B609**, 469 (2001).
[75] A. Ali and Ya. Parkhomenko, The $\eta' g^* g^*$ vertex with arbitrary gluon virtualities in the perturbative QCD hard scattering approach, Phys. Rev. D **65**, 074020 (2002).
[76] J.-K. He and Y.-D. Yang, Revisiting the radiative decays $J/\psi \to \gamma\eta^{(\prime)}$ in perturbative QCD, Nucl. Phys. **B943**, 114627 (2019).
[77] S. S. Agaev, V. M. Braun, N. Offen, F. A. Porkert, and A. Schäfer, Transition form factors $\gamma^*\gamma \to \eta$ and $\gamma^*\gamma \to \eta'$ in QCD, Phys. Rev. D **90**, 074019 (2014).
[78] R. Akhoury and J. M. Frère, η, η' mixing and anomalies, Phys. Lett. B **220**, 258 (1989).
[79] T. Feldmann, P. Kroll, and B. Stech, Mixing and decay constants of pseudoscalar mesons: The Sequel, Phys. Lett. B **449**, 339 (1999).
[80] E. B. Gregory, A. C. Irving, C. M. Richards, and C. McNeile (UKQCD Collaboration), A study of the η and η' mesons with improved staggered fermions, Phys. Rev. D **86**, 014504 (2012).
[81] C. Michael, K. Ottnad, and C. Urbach (ETM Collaboration), η and η' mixing from lattice QCD, Phys. Rev. Lett. **111**, 181602 (2013).
[82] R. Escribano, P. Masjuan, and P. Sanchez-Puertas, η and η' transition form factors from rational approximants, Phys. Rev. D **89**, 034014 (2014).
[83] R. Escribano, P. Masjuan, and P. Sanchez-Puertas, The η transition form factor from space- and time-like experimental data, Eur. Phys. J. C **75**, 414 (2015).
[84] R. Escribano, S. Gonzàlez-Solís, P. Masjuan, and P. Sanchez-Puertas, η' transition form factor from space- and timelike experimental data, Phys. Rev. D **94**, 054033 (2016).
[85] C. Urbach, Properties of flavour-singlet pseudoscalar mesons from lattice QCD, EPJ Web Conf. **134**, 04004 (2017).
[86] G. 't Hooft and M. J. G. Veltman, Scalar one loop integrals, Nucl. Phys. **B153**, 365 (1979).
[87] A. Denner, U. Nierste, and R. Scharf, A compact expression for the scalar one loop four point function, Nucl. Phys. **B367**, 637 (1991).
[88] A. Denner, Techniques for calculation of electroweak radiative corrections at the one loop level and results for W physics at LEP-200, Fortschr. Phys. **41**, 307 (1993).
[89] H. H. Patel, Package-X: A Mathematica package for the analytic calculation of one-loop integrals, Comput. Phys. Commun. **197**, 276 (2015).
[90] H. H. Patel, Package-X 2.0: A Mathematica package for the analytic calculation of one-loop integrals, Comput. Phys. Commun. **218**, 66 (2017).
[91] P. Kroll and K. Passek-Kumerički, The two gluon components of the η and η' mesons to leading twist accuracy, Phys. Rev. D **67**, 054017 (2003).
[92] P. Ball and G. W. Jones, $B \to \eta^{(\prime)}$ form factors in QCD, J. High Energy Phys. 08 (2007) 025.
[93] S. Alte, M. König, and M. Neubert, Exclusive radiative Z-boson decays to mesons with flavor-singlet components, J. High Energy Phys. 02 (2016) 162.
[94] J. J. Dudek, R. G. Edwards, and D. G. Richards, Radiative transitions in charmonium from lattice QCD, Phys. Rev. D **73**, 074507 (2006).
[95] A. V. Radyushkin, Hadronic form-factors: Perturbative QCD versus QCD sum rules, Nucl. Phys. **A532**, 141 (1991).
[96] R. Jakob and P. Kroll, The pion form-factor: Sudakov suppressions and intrinsic transverse momentum, Phys. Lett. B **315**, 463 (1993); **319**, 545(E) (1993).
[97] R. Jakob, P. Kroll, and M. Raulfs, Meson-photon transition form-factors, J. Phys. G **22**, 45 (1996).
[98] J. Bolz, P. Kroll, and G. A. Schuler, Higher Fock states and power counting in exclusive P wave quarkonium decays, Eur. Phys. J. C **2**, 705 (1998).
[99] R. L. Workman *et al.* (Particle Data Group), Review of particle physics, Prog. Theor. Exp. Phys. **2022**, 083C01 (2022).

[100] H. Negash and S. Bhatnagar, Spectroscopy of ground and excited states of pseudoscalar and vector charmonium and bottomonium, Int. J. Mod. Phys. E **25**, 1650059 (2016).
[101] S. Bhatnagar and L. Alemu, Approach to calculation of mass spectra and two-photon decays of $c\bar{c}$ mesons in the framework of Bethe-Salpeter equation, Phys. Rev. D **97**, 034021 (2018).
[102] E. Gebrehana, S. Bhatnagar, and H. Negash, Analytic approach to calculations of mass spectra and decay constants of heavy-light quarkonia in the framework of Bethe-Salpeter equation, Phys. Rev. D **100**, 054034 (2019).
[103] B. Aubert *et al.* (*BABAR* Collaboration), Measurement of the η and η' transition form-factors at $q^2 = 112$ GeV^2, Phys. Rev. D **74**, 012002 (2006).
[104] X. Jiang, F. Chen, Y. Chen, M. Gong, N. Li, Z. Liu, W. Sun, and R. Zhang, Radiative decay width of $J/\psi \to \gamma\eta_{(2)}$ from $N_f = 2$ lattice QCD, Phys. Rev. Lett. **130**, 061901 (2023).